www.czasopisma.pan.pl PAN POLSKA AKADEMIA NAUK www.journals.pan.pl

Arch. Metall. Mater. **68** (2023), 1, 81-84

DOI: https://doi.org/10.24425/amm.2023.141476

HYUNSEUNG LEE[1], HOSEONG RHEE[1], SANGSOO LEE[2], SI YOUNG CHANG[1*]

EFFECT OF BALL ON SPS CHARACTERISTICS OF Ti-Al-Nd POWDERS PREPARED BY HIGH ENERGY BALL MILLING

The effects of different types of balls on spark plasma sintering (SPS) characteristics of high energy ball milled Ti-48wt% Al-4 wt% Nd powders were investigated. After ball milling with STS balls and zirconia balls at 800 rpm for 3 h in argon atmosphere, both powders showed shape factors of about 0.8, but their average powder sizes differed respectively at approximately 11 μm and 5 μm. From XRD results, only the peaks of pure Ti, Al and Nd were detected in both powders. The obtained Ti-Al-Nd powders were consolidated by SPS technique at 1373 K for 15 min under a pressure of 50 MPa in vacuum, resulting in high density over 99%. EDS and XRD analyses indicated the formation of binary phases such as $TiAl_3$, TiAl, Ti_3Al_5, and $NdAl_3$ after SPS in both cases of STS and zirconia balls, while the ternary Ti-Al-Nd phase was detected only in the case of zirconia balls. The size of second phases was slightly smaller in the case of zirconia balls. The microhardness of the sample was 790 Hv with zirconia balls and 540 Hv with STS balls.

Keywords: High energy ball milling; STS and Zirconia ball; SPS; Ti-Al-Nd alloy; Microhardness

1. Introduction

Titanium and titanium alloys have been widely employed in industrial and biomedical applications because of their relatively low density, low modulus of elasticity, high specific strength, good biocompatibility, and corrosion resistance [1,2]. In particular, Ti-48wt% Al based alloys display excellent toughness in high temperature and exceptionally low density due to the presence of an intermetallic compound TiAl(γ). This makes them suitable for automotive engines or aircraft turbines [3-7]. Adding rare elements to a TiAl binary alloy can further increase its ductility, oxidation resistance, and hardness at high temperature [8,9]. Recently, a method was developed to successfully extract Nd, a rare earth element, from recycled NdFeB magnets [10]. This proposes a strong possibility for Nd to be used as a new alloy element for titanium alloys. However, not much is known about the effects of adding Nd on the microstructure and the mechanical properties of Ti-Al alloys.

Ti alloys can be generally manufactured by arc melting or powder metallurgy processing methods. Among these methods, high energy ball milling is an economic, simple, and yet powerful method to produce nanostructured and amorphous materials [11-14]. However, high energy ball milling can be greatly affected by the composition of the powders as well as various milling conditions. Some of the most important milling conditions are found in relation to the balls, such as their type, shape, weight, and size distribution [15,16]. Additionally, spark plasma sintering (SPS) is a novel method that enables shorter sintering durations, relatively high sintering pressures, and low temperature during sintering. These unique features lead to fine microstructure and high sintering density [17-19].

In this study, pure Ti, Al, and Nd powders are high energy ball milled with two different types of balls: STS and zirconia. The milled powders and their subsequently SPSed samples are evaluated based on their microstructures and microhardness.

2. Experimental

Pure Ti, Al, and Nd powders mixed with a weight ratio of 48:48:4 were high energy ball-milled with either STS or zirconia balls that are approximately 5.0 mm in diameter at 800 rpm for 3 h in argon atmosphere [19,20]. The obtained Ti-Al-Nd milled powders were consolidated by SPS at 1373 K for 15 min under 50 MPa pressure. The microstructures of the Ti-Al-Nd powders as well as their sintered samples were observed with an optical

[1] KOREA AEROSPACE UNIVERSITY, DEPARTMENT OF MATERIALS SCIENCE AND ENGINEERING, GOYANG, KOREA
[2] KOREA AEROSPACE UNIVERSITY, ADVANCED MATERIALS RESEARCH INSTITUTE, GOYANG, KOREA

* Corresponding author: sychang@kau.ac.kr

microscope (OM) and a scanning electron microscope (SEM). Image analysis was used to calculate the mean size and shape factor of the powders. Energy dispersive spectroscopy (EDS) and X-ray diffractometer (XRD) were utilized to analyze the components and phases of the milled powders as well as their sintered samples. The size of particles and the second phases was determined by measuring full width at half maximum (FWHM) ($= 0.9\lambda/\beta\cos\theta$, where λ is x-ray wavelength, θ is Bragg angle, β is line broadening in radians) in XRD peaks. The density of the sintered samples was measured according to the Archimedes' principle, and the micro-hardness was measured under a load of 1 kg for 10 sec.

3. Results and discussion

The SEM images of initial Ti, Al, and Nd powders are shown in Fig. 1. The initial Ti powders show irregular shapes, and the initial shapes of the Al powders are round. Their respective initial mean sizes are approximately 20 and 40 μm. In addition, the Nd powders employed in this study revealed chip typed shapes with a mean size of ~150 μm. Fig. 2 shows the SEM images and EDS analyses of the Ti-Al-Nd powder mixtures milled with STS balls and zirconia balls. The figure confirms that 46.3wt% Ti, 49.0wt% Al and 4.7wt% Nd powders are uniformly distributed after the ball milling process, which corresponds relatively well to the objective composition. It also shows that the powder size gets smaller when the ball type is changed from STS to zirconia. The mean size, shape factor, and size distribution of the milled powders are quantitatively analyzed and represented in Fig. 3. The mean powder size is approximately 11 μm with STS balls whereas it is approximately 5 μm with zirconia balls. However, the change in ball material has little effect on shape factor, as both milled powders show similar value of approximately 0.8. The size distribution of powders milled with zirconia balls is 2~20 μm, whereas, in the case of STS balls, it is between 3~30 μm. In addition, the highest number peaks of both powders well correspond to the mean powder size.

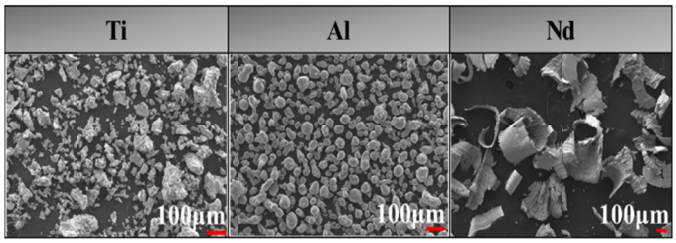

Fig. 1. SEM images of initial Ti, Al, and Nd powders

Fig. 4 demonstrates the XRD patterns of Ti-Al-Nd mixed powders each milled with STS balls and zirconia balls. Only the peaks of pure Ti, Al, and Nd are observed, which indicates no

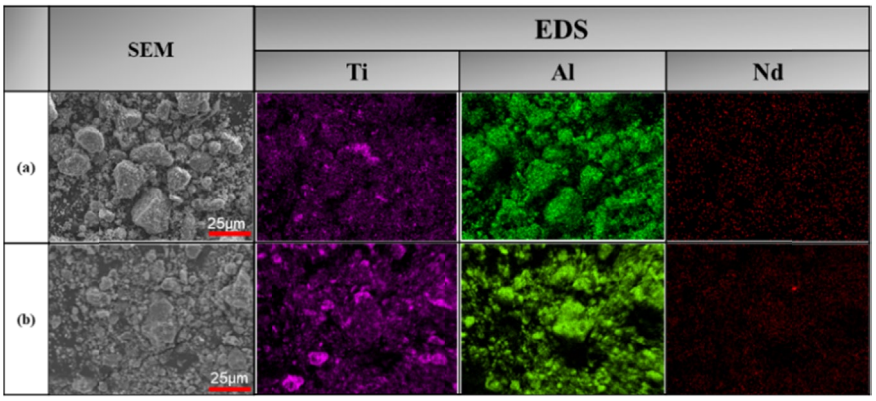

Ele. (Wt.%) \ Ball	STS	Zirconia
Ti	46.3	47.7
Al	49.0	48.1
Nd	4.7	4.2
Total	100.0	100.0

Fig. 2. SEM images & EDS analyses of mixing powders milled with (a) STS balls and (b) zirconia balls

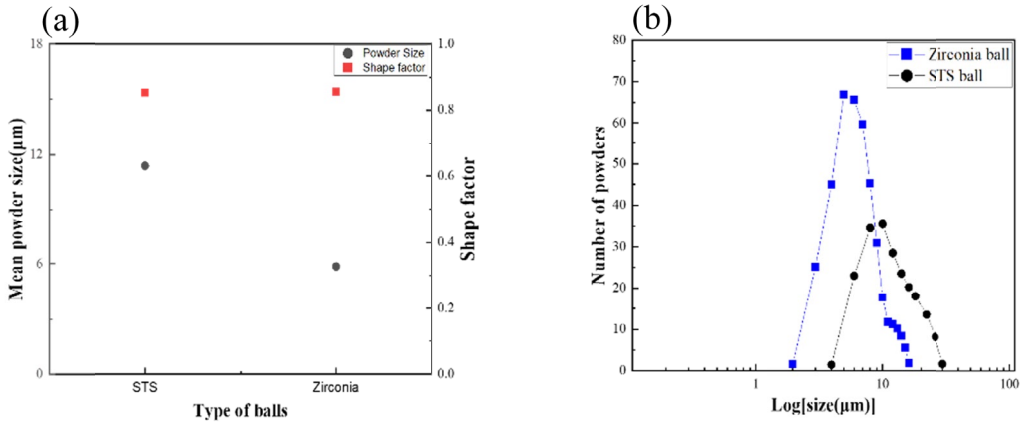

Fig. 3. (a)Mean powder size, shape factor and (b) size distribution of as-milled powders

occurrence of mechanical alloying as well as no difference in the locations of the peaks. However, the peaks appear to be wider with the use of zirconia balls, which signifies decrease in particle size. The particle size measured by FWHM is 15~20 nm in the case of zirconia balls and 18~25 nm in the case of STS balls.

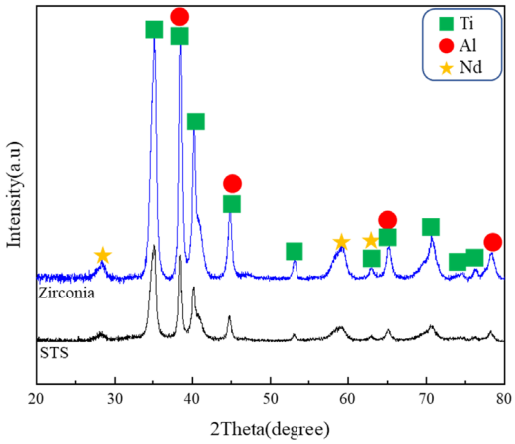

Fig. 4. XRD patterns of as milled powders

The SEM images and EDS analyses of the sintered samples are displayed in Fig. 5. No pores are found in the SEM images of both samples, allowing them to exhibit a high density of approximately 99% as listed in TABLE 1. From the EDS analysis, both sintered samples reveal uniform microstructure with relatively well-distributed 46.8wt% Ti, 49.7wt% Al and 3.5wt% Nd elements. This composition is similar to the composition of the milled powders shown in Fig. 2. The microhardness of the sintered sample is approximately 790 Hv when zirconia balls are used, whereas, in the case of STS balls, it is 540 Hv.

TABLE 1

Density and micro-hardness of as sintered samples

Type of Balls	Density (%)	Hardness (Hv)
STS	99	540
Zirconia	99	790

Fig. 6 illustrates the XRD patterns of the sintered samples using powders prepared with STS balls and zirconia balls. It is evident that the peaks of pure Ti, Al, Nd have disappeared after SPS, and also binary Ti-Al phases such as TiAl, $TiAl_3$, Ti_3Al_5, and a $NdAl_3$ phase are detected in both samples sintered with powders prepared by STS and zirconia balls. In the case of zirconia balls, in particular, the peaks of ternary $NdTi_2Al_{20}$ phase are newly detected. This is because the powders milled with zirconia balls have experienced much severer plastic deformation compared to STS balls during high energy ball milling. In the Ti-Al system, in general, there are four intermetallic compounds such as Ti_3Al, TiAl, $TiAl_2$, and $TiAl_3$ at 773 K [21]. The Ti_3Al_5 also precipitates at 973 K in the case of Al-rich TiAl alloys [22]. In addition, there are six intermetallic compounds in the Nd-Al system such as

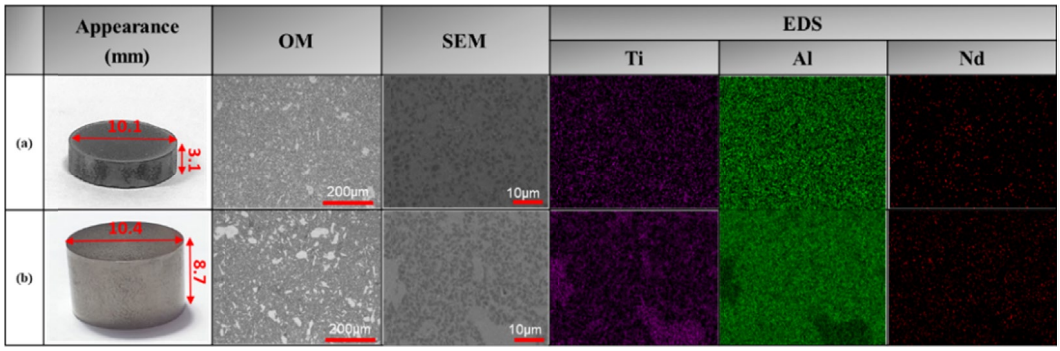

Ele. (Wt.%) \ Ball	STS	Zirconia
Ti	46.8	46.7
Al	49.7	49.5
Nd	3.5	3.8
Total	100.0	100.0

Fig. 5. SEM images and EDS analyses of sintered samples prepared with (a) STS balls and (b) zirconia balls

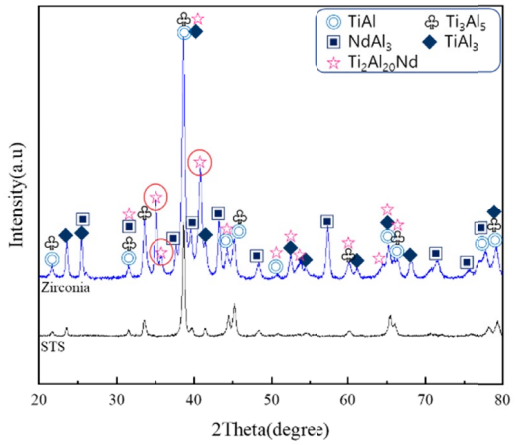

Fig. 6. XRD patterns of as-sintered samples

Nd_3Al_{11}, $NdAl_3$, $NdAl_2$, NdAl, Nd_2Al, and Nd_3Al. On the other hand, there is no intermetallic phase in the Nd-Ti binary system [21]. However, Niemann et al. [23] recently reported the existence of two Ti-Al-Nd ternary compounds such as $Nd_6Ti_4Al_{43}$ and $NdTi_2Al_{20}$. Accordingly, it is reasonably understood that the formation of TiAl, $TiAl_3$, Ti_3Al_5, $NdAl_3$ and $NdTi_2Al_{20}$ phases could be formed by the effective transfer of joule heat during SPS. The size of second phases calculated by Debye-Scherrer's equation using the half-valued width of XRD peaks is 15~30 nm, however it is decreased slightly (approximately 5 nm) with zirconia balls compared to STS balls.

As listed in Table 1, the micro hardness of the sintered sample is approximately 790 Hv when zirconia balls are used, which is much higher than 540 Hv with the use of STS balls.

This variance is believed to be due to the formation of the new ternary $NdTi_2Al_{20}$ phase along with the much finer second phases in the sample milled with zirconia balls.

4. Conclusions

Ti, 48wt% Al, and 4wt% Nd powders were ball-milled with two different types of balls, STS and zirconia, at 800 rpm for 3 hours in argon atmosphere. The mean size of the milled powders was approximately 11 μm with STS balls and approximately 5 μm with zirconia balls; however, there was no difference in the shape factor at approximately 0.8. XRD analysis detected the peaks of pure Ti, Al, and Nd in both powders. The ball-milled Ti-Al-Nd powders were consolidated by SPS at 1373 K for 15 min under a pressure of 50 MPa in vacuum. Both sintered samples had high densities over 99%. The SPSed sample that had been ball-milled with zirconia balls resulted in a micro-hardness of 790 Hv, which was much higher than 540 Hv in the case of STS balls. The binary $TiAl_3$, TiAl, Ti_3Al_5, and $NdAl_3$ phases were detected in both sintered samples, whereas the ternary Ti-Al-Nd phase existed only in the case of zirconia balls. Furthermore, the second phase sizes were smaller in using zirconia balls than STS balls. Consequently, it was reasonably concluded that the much finer second phases as well as the new ternary Ti-Al-Nd phase in the sintered sample milled with zirconia balls resulted in higher micro-hardness compared to the sample sintered with STS balls.

Acknowledgments

This work was supported by the Ministry of Trade, Industry and Energy (MOTIE, Korea) under Industrial Technology Innovation Program, No.20000970.

REFERENCES

[1] B.H. Yoon, S.H. Kim, W.S. Chang, J. Weld. Join **25**, 22-28 (2007).
[2] Y. Long, H. Zhang, T. Wang, X. Huang, Y. Li, J. Wu, H. Chen, Mat. Sci. Eng. **A 585**, 408-414 (2013).
[3] Y.W. Kim, JOM. **46** (7), 30-39 (1994).
[4] T. Matsuo, T. Nozaki, T. Asai, S. Y. Chang, M. Takeyama, Intermetallics **6**, 695-698 (1998).
[5] M. Takeyama, Y. Yamamoto, H. Morishima, K. Koike, S.Y. Chang, T. Matsuo, Mater. Sci. Eng. A **329-331**, 7 (2002).
[6] M. Es-Souni, A. Bartels, R. Wagner, Mater. Sci. Eng. A. **171**, 127-141 (1993).
[7] F. Perdix, M.F. Trichet, J.L. Bonnentien, M. Cornet, J. Bigot, Intermetallics **7**, 1323-1328 (1999).
[8] T. Kawabata, T. Tamura, O. Izumi, Metall. Trans. **24 A**, 141 (1993).
[9] Z. Yang, F. Zhang, L. Ren, R. Zhou, Z. Yu, J. Univ. Sci. Technol. Beijing **17**, 424 (1995).
[10] S.M. Park, S.W. Nam, J.Y. Cho, S.H. Lee, S.G. Hyun, T.S. Kim, Arch. Metall. Mater. **65**, 1281-1285 (2020).
[11] B. Kieback, H. Kubsch, A. Bunke, J. Phys. **IV 3**, 1425-1428 (1993).
[12] H.S. Lee, H.S. Rhee, S.S. Lee, S.Y. Chang, Korean J. Mater. Res. **31**, 677-681 (2021).
[13] S.J. Park, Y.S. Song, K.S. Nam, S.Y. Chang, J. Korea. Powd. Met. Inst. **19**, 122-126 (2012).
[14] S.Y. Chang, B.S. Kim, Y.S. Song, K.S. Nam, J. Nanosci. and Nanotech. **12**, 1353-1356 (2012).
[15] C. Suryanarayana, Prog. Mater. Sci. **46**, 1-184 (2001).
[16] M. Zakeri, M.R. Rahimipour, Adv. Powder. Technol. **23**, 31-34 (2012).
[17] R. Duan et al., Mater. Sci. Eng. **A373**, 180-186 (2004).
[18] L. Gao, H. Miyamoto, J. Inorg. Mater. **12**, 129-133 (1997).
[19] Y.R. Kim, H.S. Rhee, S.Y. Chang, Arch. Metall. Mater. **66**, 789-793 (2021).
[20] H.H. Chung, H.L. Park, J.Y. Seo, S. Y. Chang, The collected abstracts of annual autumn meeting of Materials Research Society of Korea, p. 256 (2017).
[21] H. Zhou, Q. Yao, S. Yuan, J. Alloys and Comp. **381**, 137-139 (2004).
[22] M. Doi, T. Koyama, T. Taniguchi, S. Naito, Mater. Sci. and Eng. A329-331, 891-897 (2002).
[23] S. Niemann, W. Jeitschko, J. Solid State Chem. **114**, 337-341 (1995).